

PCCP

Accepted Manuscript



This is an *Accepted Manuscript*, which has been through the Royal Society of Chemistry peer review process and has been accepted for publication.

Accepted Manuscripts are published online shortly after acceptance, before technical editing, formatting and proof reading. Using this free service, authors can make their results available to the community, in citable form, before we publish the edited article. We will replace this *Accepted Manuscript* with the edited and formatted *Advance Article* as soon as it is available.

You can find more information about *Accepted Manuscripts* in the [Information for Authors](#).

Please note that technical editing may introduce minor changes to the text and/or graphics, which may alter content. The journal's standard [Terms & Conditions](#) and the [Ethical guidelines](#) still apply. In no event shall the Royal Society of Chemistry be held responsible for any errors or omissions in this *Accepted Manuscript* or any consequences arising from the use of any information it contains.



Cite this: DOI: 10.1039/xxxxxxxxxx

Design of new disulfide-based organic compounds for the improvement of self-healing materials

Jon M. Matxain,^a José M. Asua,^b and Fernando Ruipérez^{*b}Received Date
Accepted Date

DOI: 10.1039/xxxxxxxxxx

www.rsc.org/journalname

Self-healing materials are a very promising kind of materials due to their capacity to repair themselves. Among others, diphenyl disulfide-based compounds (Ph_2S_2) appear to be among the best candidates to develop materials with optimum self-healing properties. However, few is known regarding both the reaction mechanism and the electronic structure that make possible such properties. In this vein, theoretical approaches are of great interest. In this work, we have carried out theoretical calculations on a wide set of different disulfide compounds, both aromatic and aliphatic, in order to elucidate the prevalent reaction mechanism and the necessary electronic conditions needed for improved self-healing properties. Two competitive mechanisms were considered, namely, the metathesis and the radical-mediated mechanism. According to our calculations, the radical-mediated mechanism is the responsible for this process. The formation of sulfenyl radicals strongly depends on the S-S bond strength, which can be modulated chemically by the use of proper derivatives. At this point, amino derivatives appear to be the most promising ones. In addition to the S-S bond strength, hydrogen bonding between disulfide chains seems to be relevant to favour the contact among disulfide units. This is crucial for the reaction to take place. The calculated hydrogen bonding energies are of the same order of magnitude as the S-S bond energies. Finally, reaction barriers have been analysed for some promising candidates. Two reaction mechanisms were compared, namely, the [2+2] metathesis reaction mechanism and the [2+1] radical-mediated mechanism. No computational evidence for the existence of any transition state for the metathesis mechanism was found, which indicates that the radical-mediated mechanism is the one responsible in the self-healing process of these materials. Interestingly, the calculated reaction barriers are around 10 kcal/mol regardless the substituent employed. All these results suggest that the radical formation and the structural role of the hydrogen bonding prevale over kinetics. Having this in mind, as a conclusion, some new compounds are proposed for the design of future self-healing materials with improved features.

1 Introduction

The broad interest of using reversible chemistry in materials science to synthesize reorganizable polymers has been recently established through several examples in the literature,^{1–5} where different covalent bonds are examined, exploring their poten-

tial to modify the structure of the backbones. One of the most appealing applications of reversible chemistry is the concept of self-healing materials, in which the material is able to autorepair and recover the original properties.^{6–11} Based on this reversibility, two main approaches may be devised depending on the nature of the interaction: the first one involves weak, non-covalent interactions, such as hydrogen bonds,¹² π – π stacking¹³ or metal-ion interactions,¹⁴ and the second one involves dynamic covalent bonds, for example exploiting the retro-Diels-Alder reaction.^{15–17} The main difference between these two approaches is that the use of covalent networks may provide the material with higher

^a Kimika Fakultatea, Euskal Herriko Unibertsitatea UPV/EHU and Donostia International Physics Center (DIPC), P.K. 1072, 20080 Donostia, Euskadi, Spain.

^b POLYMAT, University of the Basque Country UPV/EHU, Joxe Mari Korta Center, Avda. Tolosa 72, 20018 Donostia-San Sebastián, Spain. Tel: +34 943 018 476; E-mail: fernando.ruiperez@polymat.eu

mechanical strength and stability.

However, many reversibly covalently cross-linked polymers have inherent low reactivities that require external stimulation such as heat or UV irradiation. Thus, in order to achieve a reversible covalent self-healing material which is autonomous or needs weak stimulations, an appropriate choice of this covalent bond is a key feature.^{18–21} In this sense, disulfide bonds appear as good candidates to introduce a healing functionality at lower temperatures while keeping a reasonably level of bond strength.

The chemistry of disulfides is very versatile. Due to the dynamics and reversibility of the S-S bond cleavage (to generate sulfenyl radicals), disulfide compounds play a crucial role in several fields such as physiological chemistry, where disulfide bridges are involved in folding, conformational stability and biological activity of proteins by means of thiol-disulfide exchange reactions with the thiol moiety in cystein residues,^{22–24} or synthetic chemistry.²⁵ Besides, it is noteworthy their use in materials science as highly versatile precursors for the synthesis of colloidal nanocrystals²⁶ or as crosslinking groups that result from the vulcanization of rubber, in analogy to the role of disulfides in proteins, strongly affecting the rheology of the material.²⁷

Several disulfide compounds are shown to exchange in the presence of catalysts^{28–30} or under UV irradiation³¹ but, in order to improve their performance, it would be desirable to have this exchange at room temperature and without external stimuli. Therefore, disulfide bonds with lower bond dissociation energies are necessary to prepare self-healing materials under mild conditions. This is the case of aromatic disulfides, in which metathesis has been reported to happen at room temperature, both in solution³² and in the solid state.³³ Following this approach, a very successful work has appeared recently in the literature, where bis(4-aminophenyl) disulfide is used as a dynamic crosslinker for the design of self-healing poly(urea-urethane) elastomers, which show quantitative healing efficiency at room temperature without the need of any catalyst or external intervention.³⁴ The high healing efficiency is explained in terms of the constant exchange of aromatic disulfides at room temperature, which is further improved by the generation of hydrogen bonds among urea moieties, contributing up to a 50% of the healing efficiency.

Apart from this outstanding application, few other works are found in the literature, both theoretical^{35–37} and experimental,^{21,33,38} where the metathesis of aromatic disulfides is explored. Thus, it is clear that the mechanism of such an important and highly applicable process deserves further discussion and a more detailed investigation, to achieve a better understanding of the reaction at the molecular level, which may lead to an improvement of the self-healing capacity of the materials by predicting new disulfide bonds which experience exchange without the presence of catalysts or UV irradiation. In order to do that, theoretical methods of quantum chemistry are the most suitable

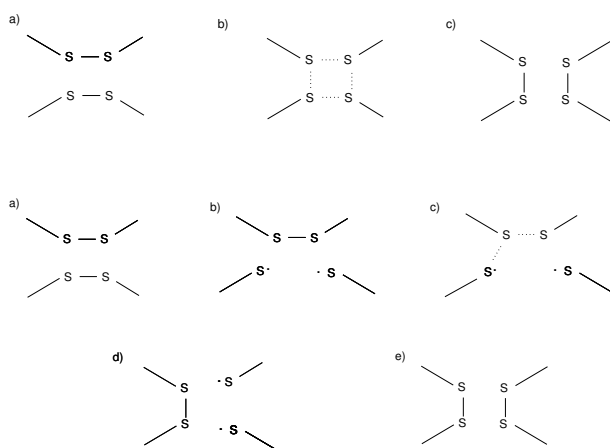


Fig. 1 Schematic representation of the [2+2] metathesis (above) and [2+1] radical mediated (below) reaction mechanisms

and useful tools to explain the phenomenology, understand the experiments and make predictions that may guide future experiments.

In this work, the self-healing process accomplished by disulfide-based materials is studied by means of theoretical chemistry, which is a very robust and useful tool for the design and study of new materials. Starting from diphenyl disulfide, several derivative compounds are designed, where different moieties (with different electron donating or withdrawing character) are introduced as substituents in the phenyl rings, in order to analyze how the substitution affects the chemistry of the process. Among these substituents, amino derivatives are found to be the most promising ones and, for these cases, the trisubstituted derivatives in *ortho* and *para* positions were considered. Besides, π -conjugated non-aromatic disulfides are also investigated. For all these compounds, the sulfur-sulfur bond dissociation energies (BDE) have been calculated to estimate the strength of this bond. The absorption energies (λ) have also been calculated to study the photodissociation of the S-S bond. In both processes, key electronic features were identified. In addition to this, the stabilization energy attained by the hydrogen bonds between disulfide chains was also evaluated. Finally, the reaction mechanism is examined by means of transition state characterization and rationalized based on the different chemical structures. Two different alternatives were considered: the [2+2] metathesis reaction mechanism and the [2+1] radical-mediated mechanism. These two mechanisms are described in Figure 1. Notice that low BDEs are compatible with both mechanisms, while photodissociation would lead to radicals that are only compatible with the radical mediated mechanism. The knowledge achieved in this analysis will allow us to propose several compounds that may be useful for the experimental community as a first step towards improved new self-healing materials.

2 Methods

All geometry optimizations were carried out in gas phase within density functional theory (DFT),^{39,40} combined with the 6-31+G(d,p) basis set.⁴¹ Harmonic vibrational frequencies were obtained by analytical differentiation of gradients, in order to determine whether the structures found are minima or transition states. The frequencies were then used to evaluate the zero-point vibrational energy (ZPVE) and the thermal (T = 298 K) vibrational corrections to the enthalpy (H) and Gibbs free energy (G) in the harmonic oscillator approximation. Single point calculations using the 6-311++G(2df,2p) basis set⁴² were performed on the optimized structures in order to refine the electronic energy, and the previously calculated corrections to the enthalpy and Gibbs free energy were used to calculate the H and G of each species, namely: $H_{TZ}^{298} = E_{TZ} + H_{DZ}^{corr,298}$ and $G_{TZ}^{298} = E_{TZ} + G_{DZ}^{corr,298}$. In order to understand the photodissociation process, Time-Dependent Density Functional Theory (TDDFT)⁴³ was used, combined with the 6-31+G(d,p) basis set. All DFT calculations were carried out using the Gaussian 09 package.⁴⁴

Wavefunction-based CASSCF/CASPT2 calculations⁴⁵⁻⁴⁹ together with the aug-cc-pVDZ basis set^{50,51} have been performed for the study of the dissociation of dimethyl disulfide and diphenyl disulfide. The active space in the methyl derivative comprises the distribution of 6 electrons in 4 orbitals, CAS(6,4), corresponding to the two σ (C-S), σ (S-S) and σ^* (S-S) orbitals. For the methyl sulfenyl radical, the active space is CAS(3,2). In the case of the phenyl compound, the π orbitals of the aromatic rings and the lone pairs in the sulfur atoms must be included in the active space, therefore, the active space is CAS(22,12) and for the phenyl sulfenyl radical, CAS(5,3). The MOLCAS 8.0 suite of programs⁵² were used throughout the study. Besides, *ab initio* Born-Oppenheimer Molecular Dynamics (QMD) calculations were further carried out for the optimized species in order to determine their thermal stability. These calculations were performed using the PBE functional,^{53,54} combined with a DZP quality basis set.⁵⁵⁻⁵⁷ The calculations were carried out at 298 K by means of the Nose-Hoover thermostat. All these simulations were as long as 40.000 a.u. (9.651 ps), with a time step of 40 a.u. (1.93 ps). These QMD calculations were performed using the TURBOMOLE package.⁵⁸

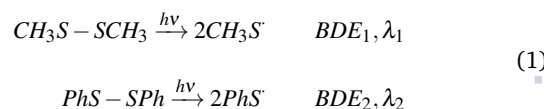
Finally, the analysis of the population of the natural orbitals have been performed using the Natural Bonding Orbital (NBO) method.⁵⁹⁻⁶¹

2.1 Benchmark of the density functionals

In order to accurately describe the homolysis of the disulfide bond, the choice of a proper density functional is a crucial step. Thus, we have selected a set of twelve popular exchange-

correlation (xc) functionals divided in five groups (see Table 1): functionals constructed within the generalized gradient approximation (GGA): PBE,^{53,54} BLYP⁶²⁻⁶⁴ and PW91;⁶⁵ hybrid GGA functionals (HGGA), such as B3LYP,^{62,66} B3LYP-D3, including the version of Grimme's dispersion with the original D3 damping function,⁶⁷ and B3P86;^{66,68} meta GGA functionals (MGGA), such as M06-L⁶⁹ and MPWB1K;⁷⁰ meta hybrid GGA functionals (MHGGA), such as M06⁷¹ and M06-2X,⁷¹ and, finally, long-range corrected (LRC) functionals, such as ω B97X-D⁷² and CAM-B3LYP.⁷³

We have tested the behaviour of these functionals in the dissociation of two model compounds: dimethyl disulfide and diphenyl disulfide, as seen in the reactions below, where the bond dissociation energy (BDE) corresponds to the enthalpy of this process calculated as: $\Delta H = 2 \times H(\text{RS}\cdot) - H(\text{RS-SR})$, where R = CH₃ for reaction 1 and R = Ph for reaction 2. λ is the absorption wavelength to the first excited state which leads to dissociation.



In Table 1, the results for the twelve density functionals together with the CASPT2 calculations and the available experimental results are shown. Since the CASPT2 results are in good agreement with the experiments, we have used them as the reference for the benchmark, since no experimental data are available for the absorption energy of the diphenyl disulfide. Therefore, the absolute errors are referred to the CASPT2 results in all cases.

It is observed that most of the functionals underestimate the bond dissociation energy, with the exception of M06-L for the dimethyl disulfide and B3LYP, B3LYP-D3, MPWB1K and M06-2X for the diphenyl disulfide. Regarding the excitation energy, all functionals overestimate this property and the deviations are greater for the diphenyl disulfide molecule.

In Table 2, where the mean absolute errors (MAE) are gathered, it can be observed that all functionals perform reasonably well in the calculation of dissociation energies, especially the MHGGA family, with a mean error of only 1.3 kcal/mol for the dissociation of dimethyl disulfide. Within this family, the most satisfactory results are provided by M06 functional (see Table 1). The functionals belonging to the GGA group show good performance too, and the results obtained with PBE and PW91 must be highlighted. LRC and HGGA functionals show a very similar performance, while the worst results are provided by the MGGA family of functionals.

In the calculation of the excitation energies, the GGA family clearly fails, with a mean error of 90.1 nm in the calculation of the absorption in the diphenyl disulfide and 30.5 nm in the dimethyl disulfide. The best results are obtained with LRC and MGGA func-

Table 1 Performance of the different DFT functionals in the calculation of the bond dissociation energy (BDE), in kcal/mol, and the excitation energy (λ) to the first excited state, in nm, for dimethyl disulfide (BDE₁, λ_1) and diphenyl disulfide (BDE₂, λ_2). In parentheses are shown the absolute errors with respect to the CASPT2 results

| Type | Functional | BDE ₁ | BDE ₂ | λ_1 | λ_2 |
|--------------|-----------------|-----------------------|---------------------|--------------------|--------------|
| GGA | PBE | 63.3 (-1.2) | 46.5 (-3.9) | 279.7 (29.4) | 398.0 (90.3) |
| | BLYP | 55.3 (-9.2) | 37.7 (-12.7) | 282.4 (32.1) | 397.5 (89.8) |
| | PW91 | 63.4 (-1.1) | 47.9 (-2.5) | 280.4 (30.1) | 398.0 (90.3) |
| HGGA | B3LYP | 55.4 (-9.1) | 57.2 (6.8) | 267.9 (17.6) | 350.3 (42.6) |
| | B3LYP-D3 | 57.6 (-6.9) | 61.7 (11.3) | 267.9 (17.6) | 350.3 (42.6) |
| | B3P86 | 61.0 (-3.5) | 46.3 (-4.1) | 265.3 (15.0) | 349.3 (41.6) |
| MGGA | M06-L | 81.1 (16.6) | 49.4 (-1.0) | 255.9 (5.6) | 362.2 (54.8) |
| | MPWB1K | 62.3 (-2.2) | 64.3 (13.9) | 257.3 (7.0) | 321.5 (13.8) |
| MHGGA | M06-2X | 62.5 (-2.0) | 65.4 (15) | 268.5 (18.2) | 334.8 (27.1) |
| | M06 | 64.0 (-0.5) | 49.1 (-1.3) | 276.5 (26.2) | 357.3 (49.6) |
| LRC | ω B97X-D | 61.0 (-3.5) | 48.0 (-2.4) | 257.9 (7.6) | 319.9 (12.2) |
| | CAM-B3LYP | 55.7 (-8.8) | 41.5 (-8.9) | 258.6 (8.3) | 319.8 (12.1) |
| CASPT2 | | 64.5 | 50.4 | 250.3 | 307.7 |
| Experimental | | 65.2±0.9 ^a | 51.2±3 ^b | 248.0 ^c | - |

^aRef. ⁷⁴, ^bRef. ⁷⁵, ^cRef. ⁷⁶

Table 2 Mean absolute error (MAE) for each family of functionals in the computation of bond dissociation energies (BDE), in kcal/mol, and excitation energies (λ), in nm, for dimethyl disulfide (BDE₁, λ_1) and diphenyl disulfide (BDE₂, λ_2)

| Type of functional | BDE ₁ | BDE ₂ | λ_1 | λ_2 |
|--------------------|------------------|------------------|-------------|-------------|
| GGA | 3.8 | 6.4 | 30.5 | 90.1 |
| HGGA | 6.5 | 7.4 | 16.7 | 42.3 |
| MGGA | 9.4 | 7.5 | 6.3 | 34.3 |
| MHGGA | 1.3 | 7.2 | 22.2 | 38.4 |
| LRC | 6.2 | 5.7 | 8.0 | 12.2 |
| MAE | 5.4 | 6.8 | 16.7 | 43.5 |

tionals. Within the first group, ω B97X-D is the functional which performs better, and within the second group is MPWB1K. However, comparing the overall performance of both functionals (see Table 1) we can state that ω B97X-D is the best functional and, therefore, will be used along the whole work, not only for geometry optimization and frequency calculations, but also for the TDDFT calculations. That is, the calculation level is: ω B97X-D/6-31+G(d,p)// ω B97X-D/6-311++G(2df,2p).

3 Results and discussion

The success of a self-healing material relies on three basic parameters at the molecular level: the liability of the disulfide bond, the presence of hydrogen bonds between polymer chains and the capability to overcome the reaction barrier easily, at room temperature. Therefore, in the next sections the results are presented and organized as follows: firstly, we study the dissociation (both thermal and photodissociation) of the S-S bond for different diphenyl disulfide model compounds, including electron donating and withdrawing moieties in the phenyl rings, and a special analysis of the amine derivatives is performed. At the end of this section, a group of disulfides where the phenyl rings are substituted by

aliphatic groups bearing conjugated double bonds is also studied. Next, in the second section, the role of the hydrogen bonds among polymeric chains is investigated and, finally, the third section is devoted to the reaction mechanism of the process, where it is observed that the radical-mediated mechanism is preferred over the metathesis. Along the whole work, we will use as reference the bare diphenyl disulfide as well as the bis(4-aminophenyl) disulfide studied in the work of Odriozola and co-workers.³⁴

3.1 Analysis of the disulfide bond cleavage

In this section we analyze the dissociation of the disulfide bond using a set of substituted diphenyl disulfide molecules, with different moieties in the phenyl rings. Several substituting groups have been chosen depending on their ability to donate or remove electron density into the aromatic ring: electron donating (EDG) or activating groups, and electron withdrawing (EWD) or deactivating groups. The effect of the nature of the substituents is studied using the bond dissociation energy (BDE), the occupation and bond order (BO) of the sulfur-sulfur bond, as well as the spin density on the sulfenyl radical generated after the cleavage (ρ_S) and the excitation energy to the first excited state (λ).

Firstly, a set of monosubstituted diphenyl disulfides, in *para* position (see Fig. 2, left panel), is investigated. Once a moiety has been selected as the best candidate for weakening the S-S bond, that is, facilitating the healing process, the same analysis is performed for a second group of trisubstituted diphenyl disulfides with the same group both in *para* and in *ortho* positions (see Fig. 2, right panel).

3.1.1 Dissociation of monosubstituted diphenyl disulfides

The effect of six electron withdrawing groups (EWG): SO₃H, F, CO-OCH₃, CF₃, CN and NO₂, and five electron donating groups (EDG): NH₂, OCH₃, CH₃, OH and O-CO-CH₃ has been studied

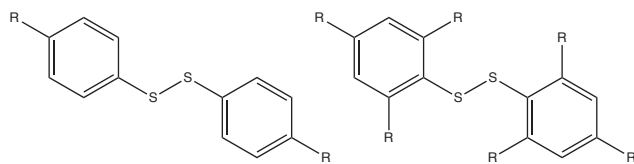


Fig. 2 Model diphenyl disulfide compounds used in the analysis of the S-S bond cleavage

and compared to the unsubstituted molecule, PhS-SPh, and with three models related to the experimentally tested amine derivative: two urea-based compounds ($R = \text{NH-CO-NH}_2$ and NH-CO-NH-CH_3), and one urethane-based model ($R = \text{O-CO-NH-CH}_3$). In Table 3 are collected the bond dissociation energy (BDE), the spin density on sulfur atom (ρ_S), the occupation of the bonding $\eta(\sigma_{SS})$ and antibonding $\eta(\sigma_{SS}^*)$ sigma orbital of the disulfide bond, as well as its bond order (BO), defined as: $(\eta(\sigma_{SS}) - \eta(\sigma_{SS}^*))/2$, the excitation energy to the first excited state (λ) and the maximum (r_{S-S}^{\max}) and average (r_{S-S}^{ave}) sulfur-sulfur bond distances obtained in the molecular dynamics simulations.

Comparing the results to the unsubstituted diphenyl disulfide, it is possible to observe that the EWGs increase both the spin density on sulfur atoms (from 0.809 in PhS-SPh to 0.852 in the cyano-substituted derivative) and the BDE (from 48.0 kcal/mol in PhS-SPh to 55.56 kcal/mol in the sulfonic acid derivative). It is remarkable how the fluorine atom, although it is a strong withdrawing moiety, has the opposite effect: the spin density is lower than in the unsubstituted disulfide (0.792 vs 0.809) and also its BDE (47.17 vs 48.00 kcal/mol). It is well known that in the halogen-substituted aromatic rings there is an electron-withdrawing effect for chlorine but there is essentially no effect for fluorine. Although the dipole moment is greater in the fluorinated phenyl because fluorine has a greater electronegativity than chlorine, the resonance effect for fluorine is also better than for chlorine because fluorine has a significant $2p-2p$ orbital overlap with carbon, while chlorine shows an inefficient $3p-2p$ overlap. In the case of fluorine, these two effects efficiently cancel out for a net dipole of essentially zero, which means that it does not exert an appreciable inductive effect. Therefore, in the fluorine-substituted diphenyl disulfide, we find values close to the ones of the unsubstituted disulfide, showing even a slightly reversed effect compared to other EWGs.

However, when the phenyl rings are substituted with an EDG, including the compound used in Ref.³⁴, we observe the opposite effect, that is, a decrease in the spin density on the sulfur atom (from 0.809 to 0.726 in the amino derivative) as well as in the BDE (from 46.62 to 41.28 kcal/mol, also in the amino derivative). It is worth emphasizing the effect of the ester group (O-CO-CH_3), which induces a greater spin density (0.840 vs 0.809) and greater BDE (48.29 vs 48.00 kcal/mol). In this moiety, the electron do-

nating resonance contribution is expected to be considerably less than the observed for OCH_3 , for example, due to the fact that the lone-pair electrons on the ester are also delocalized into the carbonyl oxygen. Similar behavior is observed in the urethane derivative (O-CO-NH-CH_3), with a spin density of 0.804 and BDE of 51.99 kcal/mol.

Regarding the occupation number of the bonding and antibonding orbitals (σ_{SS} , σ_{SS}^*) and the bond order of the S-S bond, we find, in general, that all the moieties induce a charge transfer from the bonding to the antibonding orbital, regardless of their nature, reducing the bond order, although this reduction is rather small, from 0.97 to 0.95 approximately. It is relevant how the antibonding orbital is largely populated when the phenyl is substituted with EDGs. This means that the resonance effect is actually weakening the disulfide bond, consistent with the observed reduction of the BDE values.

Concerning the results of the molecular dynamics, we find that lower bond dissociation energies are followed by longer sulfur-sulfur bond distances, as expected, which is a reflection of the easiness to cleavage the S-S bond. Thus, when EWGs are present, shorter bond distances are observed (2.25 - 2.27 Å); however, if the phenyl is substituted with EDGs, the opposite trend is noticed, where the maximum S-S bond distance is provided by the NH_2 derivative (2.41 Å). Nevertheless, this variation is not perfectly linear and probably longer time simulations would be needed to produce more accurate results. The calculated average distances are very similar to the DFT-optimized ones, as expected.

The analysis of the excitation energies (λ) shows that all compounds absorb in the near ultraviolet region of the spectrum, but it is remarkable that EWG-substituted molecules display longer absorption wavelengths. In this sense, the sulfonic moiety, which exerts an increase of the BDE of more than 7 kcal/mol with respect to the bare diphenyl disulfide, absorbs at 383.4 nm, close to the visible region of the spectrum (390 nm), which means that the photodissociation may take place easier than the thermal dissociation under room conditions. However, for the rest of the cases, the absorption wavelength is located in the UV. Therefore, under room conditions, photodissociation would not take place unless external stimulation is given.

In summary, we may conclude that the electron donating groups activate the aromatic ring and, as consequence, the following two effects are enhanced. First, the delocalization into the aromatic ring of the unpaired electron of the sulfenyl radical generated in the dissociation, which is consistent with the observed reduction of the spin density on sulfur and, thus, a stabilization effect is accomplished. Second, the increase in the electron density into the antibonding σ_{SS}^* bond, producing a weakening of the S-S bond. The combination of these two effects reduces the bond dissociation energy. Among the EDGs studied, is the amino moiety (NH_2) the one with less electron density on sulfur

Table 3 Bond dissociation energy (BDE), in kcal/mol, spin density on sulfur atom (ρ_S), occupation numbers (η) for the bonding and antibonding σ_{SS} orbitals, bond order (BO) of the disulfide bond, excitation energy (λ), in nm, and optimized sulfur-sulfur bond length (r_{S-S}^{opt}), in Å, calculated at the ω B97X-D/6-31+G(d,p)// ω B97X-D/6-31++G(2df,2p) level of theory. r_{S-S}^{max} and r_{S-S}^{ave} correspond to the maximum and average sulfur-sulfur bond distances, in Å, calculated in the QMD simulations

| R | BDE | ρ_S | $\eta(\sigma_{SS})$ | $\eta(\sigma_{SS}^*)$ | BO(σ_{SS}) | λ | r_{S-S}^{opt} | r_{S-S}^{max} | r_{S-S}^{ave} |
|-----------------------------|-------|----------|---------------------|-----------------------|---------------------|-----------|-----------------|-----------------|-----------------|
| H | 48.00 | 0.809 | 1.9792 | 0.0212 | 0.979 | 319.9 | 2.10 | 2.22 | 2.09 |
| NH-CO-NH ₂ | 46.62 | 0.775 | 1.9596 | 0.0583 | 0.957 | 340.3 | 2.11 | 2.33 | 2.13 |
| NH-CO-NH-CH ₃ | 48.55 | 0.769 | 1.9602 | 0.0578 | 0.951 | 359.9 | 2.11 | 2.31 | 2.12 |
| O-CO-NH-CH ₃ | 51.99 | 0.804 | 1.9613 | 0.0522 | 0.955 | 357.1 | 2.11 | 2.33 | 2.12 |
| Electron withdrawing groups | | | | | | | | | |
| CO-OCH ₃ | 48.83 | 0.827 | 1.9605 | 0.0489 | 0.956 | 338.4 | 2.10 | 2.26 | 2.10 |
| CN | 49.33 | 0.852 | 1.9600 | 0.0474 | 0.956 | 333.4 | 2.09 | 2.27 | 2.11 |
| CF ₃ | 50.13 | 0.837 | 1.9596 | 0.0485 | 0.956 | 334.2 | 2.10 | 2.26 | 2.10 |
| NO ₂ | 50.23 | 0.833 | 1.9596 | 0.0453 | 0.957 | 341.1 | 2.09 | 2.26 | 2.10 |
| SO ₃ H | 55.56 | 0.840 | 1.9569 | 0.0492 | 0.954 | 383.4 | 2.12 | 2.25 | 2.10 |
| F | 47.17 | 0.792 | 1.9628 | 0.0565 | 0.953 | 317.8 | 2.10 | 2.30 | 2.12 |
| Electron donating groups | | | | | | | | | |
| NH ₂ | 41.28 | 0.726 | 1.9634 | 0.0711 | 0.946 | 320.5 | 2.11 | 2.41 | 2.13 |
| OCH ₃ | 44.11 | 0.769 | 1.9607 | 0.0543 | 0.953 | 316.9 | 2.10 | 2.27 | 2.12 |
| OH | 44.63 | 0.767 | 1.9635 | 0.0638 | 0.950 | 311.3 | 2.10 | 2.31 | 2.13 |
| CH ₃ | 46.62 | 0.801 | 1.9614 | 0.0573 | 0.952 | 320.0 | 2.10 | 2.33 | 2.11 |
| O-CO-CH ₃ | 48.29 | 0.840 | 1.9607 | 0.0543 | 0.953 | 319.8 | 2.10 | 2.28 | 2.10 |

(0.726) and greater population on the σ_{SS}^* bond (0.0711), with a resulting BDE of 41.28 kcal/mol, almost 7 kcal/mol less than the unsubstituted diphenyl disulfide.

3.1.2 Dissociation of amine derivatives

The analysis performed in the previous section shows that, in order to decrease the bond dissociation energy, it is necessary to substitute the phenyl ring with an electron donating group. Since among the studied moieties the amino group (NH₂) is the most promising, producing a decrease of 6.7 kcal/mol in the BDE, in this section we intend to further improve this result by means of three approximations: first, the modification of the amino group and, second, the analysis of the effect exerted by the presence of more amino groups in the phenyl ring, specifically in *ortho* positions, to obtain bis(2,4,6-triaminophenyl) disulfides (see Figure 2, right panel). Finally, a third set of compounds will be studied, where the phenyl ring is substituted by different aliphatic conjugated double bonds. The results are summarized in Tables 4, 5 and 6.

The modification of the amine group consists in the substitution of one hydrogen atom by different moieties, among them those bearing double bonds that may increase the conjugation degree with the lone pair of the nitrogen and the phenyl ring. We have performed the same analysis as in the previous section, that is, we have calculated the bond dissociation energy (BDE), spin density on sulfur (ρ_S), occupation numbers of the bonding and antibonding σ_{SS} orbitals, the bond order (BO), excitation energy to the first excited state (λ) and dynamic simulations have been carried out as well. Concerning the monosubstituted disulfides, it is observed

that the modification of the amine moiety may either facilitate or hinder the sulfur-sulfur bond cleavage (see Table 4). In this manner, when a carbonyl group is included, the electronegativity of this group removes electron density from the nitrogen center, diminishing the ring-activating effect of the amine, and the BDE grows to values closer to the one of the bare diphenyl disulfide (48.00 kcal/mol). The introduction of groups such as vinyl (NH-CH=CH₂), methanol (NH-CH₂OH), phenyl (NH-Ph) or an extra amine group (NH-NH₂) induces slight changes on the BDE, 1-2 kcal/mol, compared to the unsubstituted amine (NH₂). Surprisingly, we observe that including an EWG in the vinyl group, such as -OH (NH-CH=CHOH), a remarkable decrease of the BDE takes place (36.73 kcal/mol).

Nevertheless, the incorporation of moieties in *ortho* positions of the phenyl ring has a remarkable effect on the bond dissociation energies and notable reductions are observed, which is also reflected in low spin density values and large populations of the antibonding σ_{SS}^* orbital (see Table 5). Hence, when three amine groups are included in the rings, denoted as (NH₂)₃ in the table, the BDE drops from 41.28 to 30.13 kcal/mol. The spin density is only 0.577, compared to 0.726 of the *para*-amine monoderivative and to 0.809 of the unsubstituted diphenyl disulfide. Also, the population of the antibonding orbital is calculated to be 0.14, twice the value of the monosubstituted compound (0.07) and almost ten times of the one corresponding to the bare diphenyl (0.02). All these facts induce the observed reduction of the BDE. Besides, modifications of the amine groups have been carried out again and, in general, minor changes are found with respect to

Table 4 Bond dissociation energy (BDE), in kcal/mol, spin density on sulfur atom (ρ_S), occupation numbers (η) for the bonding and antibonding σ_{SS} orbitals, bond order (BO) of the disulfide bond, excitation energy (λ), in nm, and optimized sulfur-sulfur bond length (r_{S-S}^{opt}), in Å, calculated at the ω B97X-D/6-31+G(d,p)// ω B97X-D/6-311++G(2df,2p) level of theory, for monosubstituted amino derivatives of diphenyl disulfide. r_{S-S}^{max} and r_{S-S}^{ave} correspond to the maximum and average sulfur-sulfur bond distances, in Å, calculated in the QMD simulations

| R | BDE | ρ_S | $\eta(\sigma_{SS})$ | $\eta(\sigma_{SS}^*)$ | BO(σ_{SS}) | λ | r_{S-S}^{opt} | r_{S-S}^{max} | r_{S-S}^{ave} |
|--------------------------------------|-------|----------|---------------------|-----------------------|---------------------|-----------|-----------------|-----------------|-----------------|
| NH ₂ | 41.28 | 0.726 | 1.9634 | 0.0711 | 0.946 | 320.5 | 2.11 | 2.41 | 2.13 |
| NH-CH=CHOH | 36.73 | 0.717 | 1.9617 | 0.0725 | 0.945 | 318.2 | 2.11 | 2.39 | 2.14 |
| NH-CH ₂ OH | 39.14 | 0.746 | 1.9598 | 0.0746 | 0.943 | 346.5 | 2.10 | 2.38 | 2.14 |
| N-(CH ₂ OH) ₂ | 39.94 | 0.761 | 1.9613 | 0.0661 | 0.948 | 317.4 | 2.10 | 2.36 | 2.12 |
| NH-CH=CH ₂ | 42.06 | 0.736 | 1.9615 | 0.0703 | 0.946 | 324.3 | 2.11 | 2.29 | 2.15 |
| NH-NH ₂ | 42.51 | 0.826 | 1.9619 | 0.0709 | 0.946 | 317.7 | 2.11 | 2.34 | 2.14 |
| NH-Ph | 42.70 | 0.730 | 1.9598 | 0.0747 | 0.943 | 366.1 | 2.13 | 2.36 | 2.15 |
| NH-COOH | 45.27 | 0.779 | 1.9620 | 0.0614 | 0.950 | 325.3 | 2.10 | 2.40 | 2.12 |
| NH-HCO | 45.81 | 0.781 | 1.9608 | 0.0587 | 0.951 | 321.1 | 2.10 | 2.28 | 2.12 |
| NH-CO-NH ₂ | 46.62 | 0.775 | 1.9596 | 0.0583 | 0.957 | 340.3 | 2.11 | 2.33 | 2.13 |
| NH-CO-NH-CH ₃ | 48.55 | 0.769 | 1.9602 | 0.0578 | 0.951 | 359.9 | 2.11 | 2.31 | 2.12 |
| N-(CO-NH ₂) ₂ | 49.03 | 0.826 | 1.9799 | 0.0184 | 0.981 | 268.0 | 2.05 | 2.28 | 2.10 |
| NH-CO-NHCl | 49.04 | 0.784 | 1.9570 | 0.0727 | 0.942 | 393.8 | 2.15 | 2.36 | 2.12 |
| NH-CHClOH | 51.61 | 0.755 | 1.9601 | 0.0630 | 0.949 | 355.4 | 2.12 | 2.43 | 2.19 |

the triamine compound, and no clear trend is observed. However, it is outstanding the results obtained with the amino-vinyl derivatives ((NH-CH=CH₂)₃ and (NH-CH=CHOH)₃), where a dramatic reduction of more than 10 kcal/mol is observed.

In order to check if this effect is exclusively due to the presence of extra substituents on the aromatic ring, independently of their nature, we have also calculated the BDE for the trihydroxy derivative, (OH)₃, since it appeared to be a good candidate among the *para*-substituted derivatives (see Table 3). However, we observe that there is no remarkable change after the addition of the two hydroxyl groups, from 44.63 to 43.71 kcal/mol. Thus, we can conclude that the reduction in the BDE is induced by the presence of activating groups close to the sulfenyl radical that stabilize it in a greater extent.

Let us analyze now the results obtained for the amino-vinyl derivatives. This notable decrease in the BDE must be attributed to the high conjugation observed in these molecules, due to the particular geometry adopted by the amino groups. In the free NH₃, the nitrogen possesses a trigonal pyramidal geometry, with a dihedral angle of 120°. Nevertheless, the NH-CH=CH₂ group adopts a more planar configuration when attached to the phenyl ring in such a way that, in the *para* position, the dihedral angle is 152° while in the *ortho* position is 176°, almost planar. This favors an extended delocalization including the lone pair of the nitrogen, the double bond of the vinyl and the aromatic ring, which is reflected in the conjugation of the π -type molecular orbitals.

3.1.3 Dissociation of non-aromatic conjugated disulfides

Finally, since the previous results point out that delocalization and conjugation are key factors for the weakening of the S-S bond, we decided to investigate different chemical structures, where the phenyl rings are substituted for other conjugated systems. Two promising compounds are [3]dendralene and thiuram disulfides.

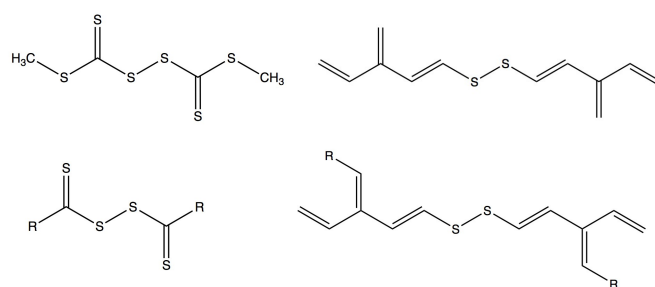


Fig. 3 Molecular structures of thiuram (top left) and [3]dendralene disulfides (top right), and the corresponding derivatives (bottom)

In figure 3 are displayed the molecular structure of these compounds and in Table 6 are collected the results corresponding to the different derivatives.

Following the analysis performed in previous sections we find that, for all [3]dendralene compounds, the spin density is notably reduced compared to both the bare diphenyl disulfide and the *para*-substituted amine derivative. Besides, the population of the antibonding σ_{SS}^* orbitals is notably increased; however, these values are below the one shown by the *para*-NH₂ derivative, except for the NH-CH₂OH compound. In any case, the dissociation energies are well below, in general, than the reference compounds in Table 6. Regarding thiuram disulfide, this molecule shows a BDE similar to the one of bare diphenyl disulfide (48.94 kcal/mol) but the substitutions improve greatly this result, which is reflected not only in the BDEs but also in the spin density and in the variation of the occupation of the bonding and antibonding σ_{SS} orbitals, as expected. It is also remarkable how the excitation energy is shifted to the visible region ($\lambda > 390$ nm) in several thiuram compounds, making them prone to experiment photodissociation more easily.

Table 5 Bond dissociation energy (BDE), in kcal/mol, spin density on sulfur atom (ρ_S), occupation numbers (η) for the bonding and antibonding σ_{SS} orbitals, bond order (BO) of the disulfide bond, excitation energy (λ), in nm, and optimized sulfur-sulfur bond length (r_{S-S}^{opt}), in Å, calculated at the ω B97X-D/6-31+G(d,p)// ω B97X-D/6-311++G(2df,2p) level of theory, for trisubstituted amino derivatives of diphenyl disulfide. r_{S-S}^{max} and r_{S-S}^{ave} correspond to the maximum and average sulfur-sulfur bond distances, in Å, calculated in the QMD simulations

| R | BDE | ρ_S | $\eta(\sigma_{SS})$ | $\eta(\sigma_{SS}^*)$ | BO(σ_{SS}) | λ | r_{S-S}^{opt} | r_{S-S}^{max} | r_{S-S}^{ave} |
|--|-------|----------|---------------------|-----------------------|---------------------|-----------|-----------------|-----------------|-----------------|
| NH ₂ | 41.28 | 0.726 | 1.9634 | 0.0711 | 0.946 | 320.5 | 2.11 | 2.41 | 2.13 |
| (NH-CH=CH ₂) ₃ | 24.81 | 0.567 | 1.9643 | 0.1262 | 0.919 | 371.4 | 2.18 | 2.86 | 2.43 |
| (NH-CH=CHOH) ₃ | 28.37 | 0.535 | 1.9653 | 0.1441 | 0.911 | 373.5 | 2.37 | 3.04 | 2.57 |
| (NH-CO-NH ₂) ₃ | 29.11 | 0.582 | 1.9643 | 0.1074 | 0.928 | 372.1 | 2.15 | 2.67 | 2.40 |
| (NH ₂) ₃ | 30.13 | 0.577 | 1.9644 | 0.1402 | 0.912 | 350.1 | 2.16 | 2.90 | 2.39 |
| (NH-Ph) ₃ | 30.23 | 0.545 | 1.9579 | 0.1225 | 0.918 | 382.3 | 2.17 | 3.23 | 2.43 |
| (NH-NH ₂) ₃ | 33.47 | 0.532 | 1.9641 | 0.1594 | 0.902 | 375.9 | 2.29 | 2.78 | 2.36 |
| (NH-HCO) ₃ | 46.35 | 0.661 | 1.9612 | 0.0901 | 0.936 | 341.3 | 2.13 | 2.51 | 2.27 |
| (OH) ₃ | 43.71 | 0.620 | 1.9617 | 0.0663 | 0.948 | 335.8 | 2.11 | 2.30 | 2.15 |
| <i>p</i> -NH-CO-NH-CH ₃ <i>o</i> -NH ₂ | 26.25 | 0.591 | 1.9665 | 0.1159 | 0.925 | 358.3 | 2.17 | 2.78 | 2.43 |
| <i>p</i> -NH-CO-NH ₂ <i>o</i> -NH ₂ | 26.46 | 0.595 | 1.9664 | 0.1156 | 0.925 | 356.6 | 2.17 | 2.61 | 2.32 |
| <i>p</i> -NH-CH ₂ OH <i>o</i> -NH ₂ | 29.74 | 0.582 | 1.9642 | 0.1359 | 0.914 | 348.0 | 2.17 | 2.69 | 2.34 |

Nevertheless, estimated photodissociation is not possible for the rest of the compounds.

In general, the [3]dendralene and thiuram disulfide derivatives show rather low bond dissociation energies, lower than those of the *para*-substituted amine derivatives and close to the trisubstituted ones, which makes them good candidates for self-healing materials based in aliphatic compounds without the need of external stimuli such as light or heat. This results open the door to new families of disulfides, which may be a promising alternative to aromatic disulfides.

Finally, as a summary, we have represented graphically in Figure 4 the relationship of the spin density and the bond order with the dissociation energy for the different sets of compounds considered in this work. A general decreasing trend of the BDE is observed when both the spin density and the bond order are decreased, which is specially notorious for the triamine derivatives.

3.2 Relevance of hydrogen bonding

As it was observed experimentally, one of the relevant aspects in the efficiency of the self-healing process is the presence of hydrogen bonds between functional groups of different polymer chains³⁴ and, hence, in this section we intend to investigate the role of this interaction in the healing mechanism. In order to do that, we evaluate the interaction energy (ΔH^{HB}) of two disulfide chains that are able to establish this kind of bonding. Since a hydrogen bond takes place when a hydrogen bound to an electronegative atom experiences attraction to other nearby electronegative atom, not all the proposed chemical models up to now are valid, and, therefore, we have selected a few representative compounds that are able to generate hydrogen bonds. Two conformations have been explored, denoted as 1 and 2 (see Fig. 6). In the first one, the chains are located in such a way that the

disulfur units are spatially near while in the latter are at longer distances. The interaction energy is, then, designated as ΔH_1^{HB} and ΔH_2^{HB} , respectively.

In Table 7 we have gathered four groups of compounds: *para*-substituted diphenyl disulfides, trisubstituted diphenyl disulfides, [3]dendralenes and thiuram disulfides, and we have calculated, for both conformations, the interaction energy due to the presence of hydrogen bonds (ΔH^{HB}) and the distances (maximum and minimum) among the sulfur atoms of different disulfide bonds (r_{S-S}^{opt}). Besides, we have performed quantum molecular dynamics that show the transformation from conformation 1 to conformation 2. Notice that r_{S-S}^{min} coincides, approximately, with the shortest distance in conformation 1 and r_{S-S}^{max} with the longest distance in conformation 2.

The first three lines in the table correspond to the urea- and urethane-based diphenyl disulfides, with R= NH-CO-NH₂, NH-CO-NH-CH₃ and O-CO-NH-CH₃. The interaction energy due to the hydrogen bonding in these compounds varies between 30.40 and 36.89 kcal/mol for the conformation 1, and between 25.41 and 33.91 kcal/mol for the conformation 2, so that, this stabilization energy is very similar in both conformations. The quantum molecular dynamics for this system show that the position of the pair of S-S bonds oscillates between 6.5 and 14.3 Å. In Figure 5 are represented the results of the molecular dynamics performed for this system, where the top graphic shows this variation of the S-S distance among the four S atoms, and the bottom graphic represents the S-S bond distance in a single molecule, oscillating between 2.05 and 2.4 Å.

In the following three compounds it is observed that the vinyl alcohol establish a weaker interaction (close to 20 kcal/mol) with a second chain. That is, the hydrogen bonding is less effective than in the amide, acid or methyl alcohol derivatives, which

Table 6 Bond dissociation energy (BDE), in kcal/mol, spin density on sulfur atom (ρ_S), occupation numbers (η) for the bonding and antibonding σ_{SS} orbitals, bond order (BO) of disulfide bond, excitation energy (λ), in nm, and optimized sulfur-sulfur bond length (r_{S-S}^{opt}), in Å, calculated at the ω B97X-D/6-31+G(d,p)// ω B97X-D/6-311++G(2df,2p) level of theory for thiuram and dendralene. r_{S-S}^{max} and r_{S-S}^{ave} correspond to the maximum and average sulfur-sulfur bond distances, in Å, calculated in the QMD simulations

| R | BDE | ρ_S | $\eta(\sigma_{SS})$ | $\eta(\sigma_{SS}^*)$ | BO(σ_{SS}) | λ | r_{S-S}^{opt} | r_{S-S}^{max} | r_{S-S}^{ave} |
|--|-------|----------|---------------------|-----------------------|---------------------|-----------|-----------------|-----------------|-----------------|
| PhS-SPh | 48.00 | 0.809 | 1.9792 | 0.0212 | 0.979 | 319.9 | 2.10 | 2.22 | 2.09 |
| NH ₂ PhS-SPhNH ₂ | 41.28 | 0.726 | 1.9634 | 0.0711 | 0.946 | 320.5 | 2.11 | 2.41 | 2.13 |
| [3]dendralene | 38.74 | 0.642 | 1.9717 | 0.0418 | 0.965 | 295.6 | 2.08 | 2.24 | 2.12 |
| NH-CH ₂ OH | 33.78 | 0.563 | 1.9605 | 0.0795 | 0.941 | 348.1 | 2.09 | 2.42 | 2.17 |
| NH-CH=CH ₂ | 35.45 | 0.572 | 1.9662 | 0.0622 | 0.952 | 327.0 | 2.09 | 2.34 | 2.15 |
| NH-CH=CHOH | 35.49 | 0.553 | 1.9697 | 0.0633 | 0.953 | 375.1 | 2.10 | 2.36 | 2.17 |
| NH-CO-NH ₂ | 41.65 | 0.617 | 1.9700 | 0.0474 | 0.961 | 305.2 | 2.09 | 2.41 | 2.14 |
| NH-COOH | 50.53 | 0.628 | 1.9706 | 0.0441 | 0.963 | 301.8 | 2.08 | 2.35 | 2.14 |
| Thiuram | 48.94 | 0.520 | 1.9812 | 0.0458 | 0.968 | 474.5 | 2.06 | 2.31 | 2.12 |
| NH-CO-NH ₂ | 35.17 | 0.330 | 1.9768 | 0.0749 | 0.951 | 410.9 | 2.05 | 2.41 | 2.16 |
| NH-COOH | 36.72 | 0.479 | 1.9773 | 0.0661 | 0.956 | 407.5 | 2.06 | 2.32 | 2.12 |
| NH-CH ₂ OH | 40.22 | 0.513 | 1.9730 | 0.0536 | 0.960 | 354.1 | 2.07 | 2.33 | 2.13 |
| NH-CH=CH ₂ | 40.68 | 0.542 | 1.9762 | 0.0649 | 0.956 | 369.5 | 2.07 | 2.41 | 2.19 |
| NH-CH=CHOH | 47.51 | 0.542 | 1.9767 | 0.0621 | 0.953 | 359.5 | 2.06 | 2.33 | 2.15 |

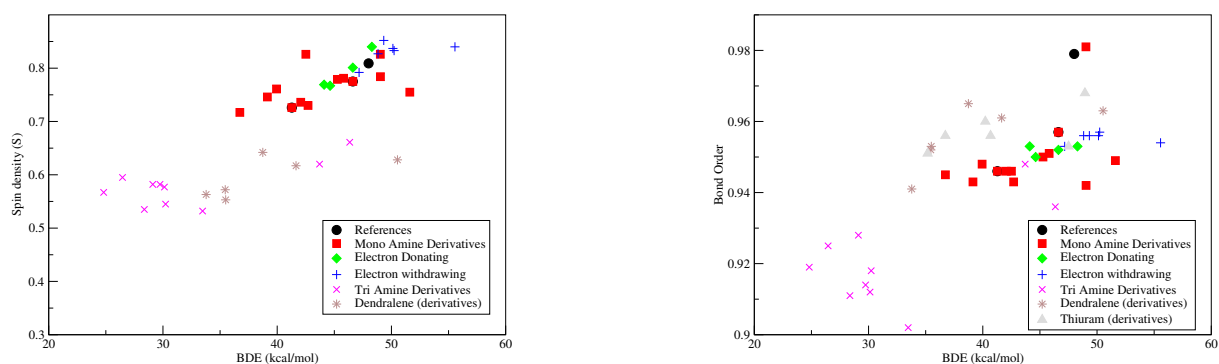


Fig. 4 Graphical representation of the spin density (left panel) and bond order (right panel) vs bond dissociation energy (BDE)

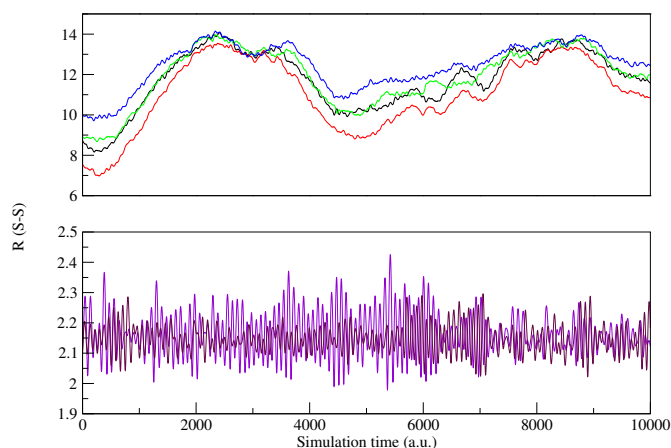


Fig. 5 Quantum molecular dynamics for the interaction of the two disulfide chains in the $(\text{NH}_2\text{-CO-NH-Ph})_2\text{S}_2$ compound. Top: sulfur-sulfur distances between the four sulfur atoms. Bottom: sulfur-sulfur distance of the disulfide bond in one of the chains

show an interaction energy between 25 and 37 kcal/mol, approximately.

For the group of trisubstituted diphenyl disulfides, we have chosen the urea (NH-CO-NH_2 , NH-CO-NH-CH_3) and the alcohol ($\text{NH-CH}_2\text{OH}$) *para*-substituted molecules, and two NH_2 groups have been added in *ortho* positions. It is remarkable how the inclusion of the amino groups in *ortho* increases the interaction energy due to the hydrogen bonding around 20 kcal/mol for both NH-CO-NH_2 and NH-CO-NH-CH_3 derivatives (53.19 and 52.98 kcal/mol, respectively), while for the the alcohol a small decrease is observed (24.86 kcal/mol).

Among [3]dendralene compounds, the unsubstituted molecule shows a small interaction energy (9.93 kcal/mol) and the second conformation could not be found. Thus, in the molecular dynamics, the dimer is not stable and tends to separate from each other, consistent with the high value of $r_{\text{S-S}}^{\text{max}} = 18.0 \text{ \AA}$. When this molecule is modified with a vinyl alcohol, an interaction energy of 14.16 kcal/mol is calculated, close to the value obtained for the *para*-substituted vinyl alcohol (19.64 kcal/mol). However, the methyl alcohol derivative shows a much greater stabilization energy (45.34 kcal/mol).

Finally, regarding thiuram compounds, the bare molecule has a similar behavior as the unsubstituted [3]dendralene, with a very low stabilization energy (1.52 kcal/mol) and the second conformation was not found. Again, the $r_{\text{S-S}}^{\text{max}}$ calculated in the molecular dynamics shows that the dimer tends to separate. The amide derivative shows an interaction energy of 37.45 kcal/mol, very similar to the amide *para*-substituted diphenyl disulfide (36.89 kcal/mol).

As a summary, we may assert that the hydrogen bonds play a structural role, which may favor the reactivity. However, at this

level of theory where only two chains are considered, is not possible to conclude that stronger hydrogen bond interactions will accomplish an improvement of the reactivity among disulfides. A higher-scale simulation, where a certain number of chains should be included, would be needed to establish a relationship between hydrogen bonding and reactivity.

3.3 Radical reaction mechanism

Finally, in order to understand the healing process, it is mandatory to study in detail the reaction mechanisms that are involved. The efficiency of the material implies that the reaction may take place spontaneously at room temperature, so that, it must fulfill, at least, the following two conditions: firstly, the cleavage of the bond should be reversible and, secondly, the reaction should have a low energy barrier, that is, the reaction path should go through a low-lying transition state in order to have a process kinetically favorable.

In this context, two reaction mechanisms have been considered in this section: the metathesis reaction mechanism based in the metathesis proposed in Odriozola's work,³⁴ and the radical-mediated reaction mechanism. In the first case, the breaking and formation of the two S-S bonds would occur simultaneously, while in the radical-mediated mechanism, the breaking of one S-S would lead to the formation of sulfur-centered radicals that eventually would attack other S-S bonds. All attempts to locate the transition state structures of metathesis reaction mechanisms failed. We therefore conclude that the occurring reaction mechanism is the radical-mediated [2+1] mechanism, where the cleavage of a S-S bond generates sulfenyl radicals that may attack another disulfide bond of a different chain through a three-membered transition state, producing a new radical, in a single-displacement reaction, and another disulfide compound.

An schematic reaction profile for this mechanism is depicted in Figure 7, where two reaction pathways have been characterized for the NH-CO-NH_2 *para*-derivative, and two different hydrogen bonding patterns between the amide moieties are considered. In black lines, the reaction mechanism occurs through complexes and transition states containing hydrogen bonds among the three chains, forming a sort of triangle. In blue lines, hydrogen bonds are established only between the central and terminal chains, in an linear path. The reaction model is the following: in an initial step, a radical monosulfide species approaches a disulfide molecule (left structure) to react via a transition state (central structure) where the radical attacks to form a new disulfide bond and generate a new monosulfide radical (right structure). The numbers correspond to enthalpy reaction energies (ΔH), which means that the transition states are located around 10 kcal/mol over the initial complex, and the energy difference between complexes is 0 or close to 0 (reversible reaction). These are approximate

Table 7 Interaction energy between two disulfide units (RS-SR) due to the presence of hydrogen bonds in conformations 1 (ΔH_1^{HB}) and 2 (ΔH_2^{HB}), in kcal/mol. r_{SS} states for the minimum and maximum S-S distance among the four S atoms in each configuration, in Å, while r_{SS}^{min} and r_{SS}^{max} are the same distances calculated in the QMD simulations

| R | Conformation 1 | | Conformation 2 | | QMD | |
|--|-------------------|-----------------|-------------------|-----------------|-----------------|-----------------|
| | ΔH_1^{HB} | r_{S-S}^{opt} | ΔH_2^{HB} | r_{S-S}^{opt} | r_{S-S}^{min} | r_{S-S}^{max} |
| NH-CO-NH ₂ | 36.89 | 7.54 - 9.98 | 33.91 | 12.61 - 13.42 | 7.0 | 14.3 |
| NH-CO-NH-CH ₃ | 30.40 | 7.72 - 9.93 | 25.41 | 12.33 - 13.01 | 6.5 | 13.8 |
| O-CO-NH-CH ₃ | 33.64 | 9.22 - 9.87 | 26.45 | 11.56 - 12.67 | 8.4 | 14.1 |
| NH-COOH | 24.79 | 7.82 - 10.00 | 27.22 | 13.54 - 14.17 | 7.8 | 15.6 |
| NH-CH ₂ OH | 29.70 | 5.85 - 7.79 | 27.86 | 12.25 - 12.72 | 5.3 | 15.5 |
| NH-CH=CHOH | 19.64 | 6.70 - 9.82 | 15.05 | 11.63 - 13.64 | 6.3 | 14.5 |
| <i>p</i> -NH-CO-NH ₂ <i>o</i> -NH ₂ | 53.19 | 7.89 - 9.92 | 49.01 | 13.61 - 13.82 | 7.2 | 12.4 |
| <i>p</i> -NH-CO-NH-CH ₃ <i>o</i> -NH ₂ | 52.98 | 7.71 - 9.74 | 49.26 | 10.66 - 11.66 | 7.7 | 11.8 |
| <i>p</i> -NH-CH ₂ OH <i>o</i> -NH ₂ | 24.86 | 8.07 - 8.86 | 27.61 | 11.75 - 13.36 | 7.1 | 10.5 |
| [3]dendralene | 9.93 | 4.92 - 7.13 | - | - | 3.5 | 18.0 |
| D-NH-CH ₂ OH | 45.34 | 5.72 - 7.55 | 41.80 | 7.24 - 8.74 | 4.5 | 9.3 |
| D-NH-CH=CHOH | 14.16 | 5.12 - 7.72 | 17.67 | 8.79 - 10.17 | 4.5 | 12.3 9 |
| Thiuram | 1.52 | 3.89 - 6.20 | - | - | 3.0 | 17.0 |
| T-NH-CO-NH ₂ | 37.45 | 4.44 - 7.13 | 34.26 | 5.44 - 6.32 | 4.0 | 9.8 |
| T-NH-COOH | 18.04 | 3.78 - 6.56 | 23.09 | 4.81 - 7.31 | 4.8 | 10.1 |

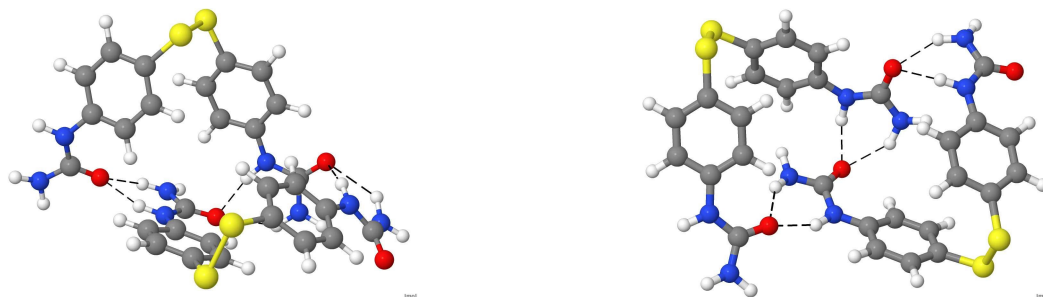


Fig. 6 Molecular structure of two *para*-substituted diphenyl disulfides (R = NH-CO-NH₂) interacting via hydrogen bonds. Conformations 1 (left) and 2 (right) are shown

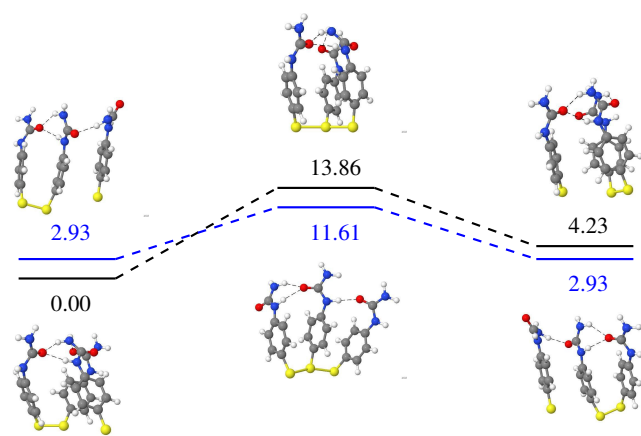


Fig. 7 [2+1] reaction mechanism proposed in this work for the NH-CO-NH₂ *para*-substituted diphenyl disulfide. ΔH values in kcal/mol. Black lines: triangular reaction path. Blue lines: linear reaction path

values, and a whole conformational analysis would be needed in order to get absolute energy values, which would be highly demanding computationally and is out of the scope of this work. Since both reaction paths are very similar, the rest of the reactions studied are done using the linear conformation.

Thus, we have studied the reaction profile for selected disulfides and, in Table 8, the geometrical parameters (sulfur-sulfur distances and angles) for the reaction complex and the transition state, as well as the reaction barrier enthalpies and imaginary frequencies of the transition state are given. This imaginary frequency corresponds to a S₁-S₂-S₃ bond stretching. Four groups of molecules have been studied: the bare diphenyl disulfide and the amino monoderivative (R = NH₂); several amine monoderivatives together with the urea- and urethane-based compounds; trisubstituted molecules and dendralene derivatives. The thiu-ram molecules have not been included since the breaking of the disulfide bond generates a radical which is delocalized between the two sulfur atoms directly bonded to the carbon, becoming indistinguishable and making the reaction mechanism less obvious.

The analysis of the S₁-S₂ and S₂-S₃ bond distances reveals that, in the transition state structure, both values are very similar, which means that the original disulfide bond is weakened (the bond distances $r_{S_1-S_2}$ are enlarged around 0.2 - 0.3 Å) and a new disulfide bond is forming (the values $r_{S_2-S_3}$ are shortened more than 1 Å in all cases). It is remarkable how all the reaction barriers (ΔH^{TS}) show a similar energy range, less than 14 kcal/mol in most cases, except for the two [3]dendralene species, with 17.24 kcal/mol for the methyl alcohol derivative and 26.97 kcal/mol for the vinyl alcohol derivative. We may highlight the low values for the bare diphenyl disulfide (9.15 kcal/mol), the NH-CO-NH-CH₃ derivative (9.73 kcal/mol) and the trisubstituted *p*-NH-CO-NH₂ *o*-NH₂ compound (9.79 kcal/mol). These results suggest that,

in almost all cases, the reaction barrier is low enough to be surpassed in normal conditions and, therefore, the reaction is not kinetically hindered.

Although the conclusion of this section implies that the main reaction mechanism goes through the formation of sulfenyl radicals and three-membered transition states, an experimental proof (such as EPR measurements, for example) would be desirable.

4 Conclusions and future work

As a summary, we may conclude that the chemical structure of the disulfide is a key factor in order to improve the properties of self-healing materials. There are two main features that are relevant for the performance of this class of materials. Firstly, the breaking of the S-S bond, which starts the process and should be spontaneous at room temperatures. This implies low bond dissociation energies or photodissociation in the visible region of the spectrum. Secondly, low energy barriers are mandatory to have the simultaneous formation and breaking of S-S bonds, in a reversible process. In this vein, theoretical methods of quantum chemistry have been used in order to rationalize the process at the molecular level, in an attempt to have a guidance for the improvement of the performance of these materials.

Three properties have been studied in detail: the S-S bond cleavage, the interaction among chains via hydrogen bonding and the reaction mechanism. In this manner, it is observed that the performance of aromatic disulfides, which have shown to be very efficient, may be enhanced by chemical modification of the aromatic rings. When the phenyl groups are *para*-substituted with ring-activating moieties, the bond dissociation energy is decreased, as a consequence of two factors: firstly, the reduction of the spin density on the sulfur atom in the generated radical, which is largely delocalized in the aromatic ring and, therefore, stabilized. Secondly, the increase of the population of the anti-bonding σ_{SS}^* orbital, reducing the bond order and promoting the bond cleavage. Besides, this weakening effect is enlarged by further substitutions in *ortho* positions with moieties that contribute to an additional delocalization of the radical electron.

The study of hydrogen bonding between chains has revealed that this interaction has a structural role in the process, keeping the disulfide chains close. However, due to the small models used in these work, is not possible to conclude that this interaction would raise the possibility of reaction.

The plausible mechanism of the reaction is a radical-mediated [2+1] mechanism. All the attempts to describe the reaction as a methatesis have been unsuccessful. The transition states have been characterized and found to be located at relatively low energies (less than 14 kcal/mol) for almost all the proposed molecules. This implies that the kinetic barriers are low for the systems studied, and easy to surpass. The radical formation, necessary at the first stage of this reaction mechanism, would basi-

Table 8 Geometrical and energetical parameters along the radical-mediated [2+1] reaction mechanism. Sulfur-sulfur distances ($r_{S_1-S_2}$ and $r_{S_2-S_3}$), in Å, (S_1, S_2, S_3) angle (α), in degrees, reaction enthalpy (ΔH^{TS}), in kcal/mol, and frequency of the imaginary mode ($\bar{\nu}$), in cm^{-1}

| R | Complex | | | Transition state | | | ΔH^{TS} | $\bar{\nu}$ |
|--|---------------|---------------|----------|------------------|---------------|----------|-----------------|-------------|
| | $r_{S_1-S_2}$ | $r_{S_2-S_3}$ | α | $r_{S_1-S_2}$ | $r_{S_2-S_3}$ | α | | |
| Ph-SS-Ph | 2.10 | 3.59 | 140.4 | 2.33 | 2.35 | 149.8 | 9.15 | -312.8 |
| NH ₂ | 2.10 | 4.13 | 158.4 | 2.40 | 2.44 | 152.4 | 13.84 | -345.4 |
| NH-CO-NH ₂ | 2.14 | 4.47 | 149.3 | 2.43 | 2.44 | 156.2 | 11.61 | -347.5 |
| NH-CO-NH-CH ₃ | 2.14 | 4.58 | 147.9 | 2.44 | 2.44 | 156.4 | 9.73 | -348.6 |
| O-CO-NH-CH ₃ | 2.14 | 4.42 | 152.9 | 2.40 | 2.42 | 151.9 | 10.62 | -335.8 |
| NH-CH ₂ OH | 2.11 | 3.73 | 164.5 | 2.39 | 2.44 | 152.9 | 12.90 | -345.7 |
| NH-COOH | 2.14 | 4.31 | 165.6 | 2.40 | 2.42 | 154.7 | 12.86 | -339.1 |
| NH-CH=CHOH | 2.15 | 4.05 | 156.8 | 2.41 | 2.46 | 154.8 | 13.06 | -357.5 |
| <i>p</i> -NH-CO-NH ₂ <i>o</i> -NH ₂ | 2.20 | 4.03 | 142.1 | 2.57 | 2.66 | 171.6 | 9.79 | -327.4 |
| <i>p</i> -NH-CO-NH-CH ₃ <i>o</i> -NH ₂ | 2.20 | 4.19 | 141.5 | 2.57 | 2.66 | 171.5 | 11.24 | -328.5 |
| <i>p</i> -NH-CH ₂ OH <i>o</i> -NH ₂ | 2.16 | 3.88 | 151.8 | 2.64 | 2.66 | 170.9 | 11.50 | -327.7 |
| D-NH-CH ₂ OH | 2.12 | 4.31 | 110.7 | 2.41 | 2.41 | 142.9 | 17.24 | -408.6 |
| D-NH-CH=CHOH | 2.09 | 3.81 | 176.4 | 2.52 | 2.44 | 149.0 | 26.97 | -389.2 |

cally occur due to thermal dissociation of the S-S bond, and not due to photodissociation, since the absorption wavelengths correspond to the UV region in most cases. Hence, photodissociation only would take place under external stimulation of the material.

Besides, since the delocalization of the radical and π -conjugation are relevant factors to control the strength of the disulfide bridge, new alternatives such as conjugated aliphatic structures have been explored. In particular, thiuram and [3]dendralene disulfides have been studied and the results show that these compounds possess very low dissociation energies and are good candidates for self-healing materials. This result is of high relevance, since aliphatic disulfides usually need an external stimulus, such as heat or light, to work efficiently, but the results provided in this work open the possibility to use aliphatic compounds that are even more efficient than the usual diphenyl-based compounds. Regarding the reaction mechanism, it is observed that the reaction barriers of [3]dendralene derivatives are higher compared with those of the aromatic disulfides, while the case of thiuram has not been calculated, since its particular molecular structure makes the reaction mechanism to be more complicated, and further studies must be performed. This would be the main drawback of using aliphatic disulfides.

Based on the results obtained in this study, we may propose several candidates that may enhance the properties of these important materials. Among the aromatic disulfides, an outstanding performance is carried out by the trisubstituted urea derivatives: *p*-NH-CO-NH₂ *o*-NH₂ and *p*-NH-CO-NH-CH₃ *o*-NH₂, where the presence of the NH₂ moieties in *ortho* positions of the ring seems to improve the behavior. Also, the change of the amide group by a methyl alcohol substituted amine, *p*-NH-CH₂OH *o*-NH₂ performs very satisfactorily. The same alcohol without *ortho* substituents

is also very promising: *p*-NH-CH₂OH. Among the aliphatic compounds, the following [3]dendralene: D-NH-CH₂OH and thiuram: T-NH-CO-NH₂ are very promising as an alternative to aromatic compounds.

Finally, in order to surpass the limitations associated to the use of small models and to get a more general interpretation of the observed phenomena, further molecular dynamics simulations based on several candidates selected from this work are already on-going in our laboratory, making use of larger, more realistic models, to study the role of hydrogen bonding in the interaction and reactivity among disulfide chains, as well as the possibility to establish additional interactions such as π - π stacking between aromatic rings.

Acknowledgments

Technical and human support provided by IZO-SGI, SGIker (UPV/EHU, MICINN, GV/EJ, ERDF and ESF) is gratefully acknowledged for assistance and generous allocation of computational resources.

References

- 1 J. W. Kamplain and C. W. Bielawski, *Chem. Commun.*, 2006, 1727.
- 2 Y. Ruff and J.-M. Lehn, *Biopolymers*, 2008, **89**, 486.
- 3 H. Otsuka, T. Muta, M. Sakada, T. Maeda and A. Takahara, *Chem. Commun.*, 2009, 1073.
- 4 Y. Amamoto, T. Maeda, M. Kikuchi, H. Otsuka and A. Takahara, *Chem. Commun.*, 2009, 689.
- 5 T. Maeda, H. Otsuka and A. Takahara, *Prog. Polym. Sci.*, 2009, **34**, 581.
- 6 D. Y. Wu, S. Meure and D. Solomon, *Prog. Polym. Sci.*, 2008, **33**, 479.

- 7 S. D. Bergman and F. Wudl, *J. Mater. Chem.*, 2008, **18**, 41.
- 8 T. C. Mauldin and M. R. Kessler, *Int. Mater. Rev.*, 2010, **55**, 317.
- 9 J. A. Syrett, C. R. Becer and D. M. Haddleton, *Polym. Chem.*, 2010, **1**, 978.
- 10 S. Burattini, B. W. Greenland, D. Chappell, H. M. Colquhoun and W. Hayes, *Chem. Soc. Rev.*, 2010, **39**, 1973.
- 11 N. K. Guimard, K. K. Oehlenschlaeger, J. Zhou, S. Hilf, F. G. Schmidt and C. Barner-Kowollik, *Macromol. Chem. Phys.*, 2012, **213**, 131.
- 12 P. Cordier, F. Tournilhac, C. Soulie-Ziakovic and L. Leibler, *Nature*, 2008, **451**, 977.
- 13 S. Burattini, H. M. Colquhoun, J. D. Fox, D. Friedmann, B. W. Greenland, P. J. F. Harris, W. Hayes, M. E. Mackay and S. J. Rowan, *Chem. Commun.*, 2009, 6717.
- 14 M. Burnworth, L. M. Tang, J. R. Kumpfer, A. J. Duncan, F. L. Beyer, G. L. Fiore, S. J. Rowan and C. Weder, *Nature*, 2011, **472**, 334.
- 15 X. Chen, M. A. Dam, K. Ono, A. Mal, H. Shen, S. R. Nutt, K. Sheran and F. Wudl, *Science*, 2002, **295**, 1698.
- 16 X. Chen, F. Wudl, A. K. Mal, H. Shen and S. R. Nutt, *Macromolecules*, 2003, **36**, 1802.
- 17 Y.-L. Liu and Y.-W. Chen, *Macromol. Chem. Phys.*, 2007, **208**, 224.
- 18 G. H. Deng, C. M. Tang, F. Y. Li, H. F. Yiang and Y. M. Chen, *Macromolecules*, 2010, **43**, 1191.
- 19 K. Imato, M. Nishihara, T. Kanehara, Y. Amamoto, A. Takahara and H. Otsuka, *Angew. Chem. Int. Ed.*, 2012, **51**, 1138.
- 20 P. Zheng and T. J. McCarthy, *J. Amer. Chem. Soc.*, 2012, **134**, 2024.
- 21 Y. Amamoto, H. Otsuka, A. Takahara and K. Matyjaszewski, *Adv. Mater.*, 2012, **24**, 3975.
- 22 D. Ritz and J. Beckwith, *Annu. Rev. Microbiol.*, 2001, **55**, 21.
- 23 Y. H. Kim, in *Organic Sulfur Chemistry: Biochemical Aspects*, ed. S. Oae and T. Okuyama, CRC Press, Boca Raton, 1992, ch. 4.
- 24 W. J. Wedemeyer, E. Welker, M. Narayan and H. A. Scheraga, *Biochemistry*, 2000, **39**, 4207.
- 25 S. Oae, in *Organic Sulfur Chemistry: Structure and Mechanism*, CRC Press: Boca Raton, 1991.
- 26 Y. Guo, S. R. Alvarado, J. D. Barclay and J. Vela, *ACS Nano*, 2013, **7**, 3616.
- 27 W. Hoffmann, in *Vulcanization and Vulcanizing Agents*, MacLaren, London, 1967.
- 28 J. A. Yoon, J. Kamada, K. Koynov, J. Mohin, R. Nicolaj, Y. Zhang, A. C. Balazs, T. Kowalewski and K. Matyjaszewski, *Macromolecules*, 2012, **45**, 142.
- 29 N. V. Tsarevsky and K. Matyjaszewski, *Macromolecules*, 2002, **35**, 9009.
- 30 J. K. Oh, C. B. Tang, H. F. Gao, N. V. Tsarevsky and K. Matyjaszewski, *J. Amer. Chem. Soc.*, 2006, **128**, 5578.
- 31 H. Otsuka, S. Nagano, Y. Kobashi, T. Maeda and A. Takahara, *Chem. Commun.*, 2010, **46**, 1150.
- 32 R. J. Sarma, S. Otto and J. R. Nitschke, *Chem.-Eur. J.*, 2007, **13**, 9542.
- 33 A. M. Belenguer, T. Frišćić, G. M. Day and J. K. M. Sanders, *Chem. Sci.*, 2011, **2**, 696.
- 34 A. Rekondo, R. Martin, A. Ruiz de Luzuriaga, G. Cabañero, H. J. Grande and I. Odriozola, *Mater. Horiz.*, 2014, **1**, 237.
- 35 R. Benassi, G. L. Fiandri and F. Taddei, *Tetrahedron*, 1994, **50**, 12469.
- 36 L.-F. Zou, Y. Fu, K. Shen and Q.-X. Guo, *J. Mol. Struct.: THEOCHEM*, 2007, **807**, 87.
- 37 A. Modelli and D. Jones, *J. Phys. Chem. A*, 2006, **110**, 10219.
- 38 J. Canadell, H. Goossens and B. Klumperman, *Macromolecules*, 2011, **44**, 2536.
- 39 P. Hohenberg and W. Kohn, *Phys. Rev.*, 1964, **136**, B864.
- 40 W. Kohn and L. J. Sham, *Phys. Rev.*, 1965, **140**, A1133.
- 41 W. J. Hehre, R. Ditchfield and J. A. Pople, *J. Chem. Phys.*, 1972, **56**, 2257.
- 42 R. Krishnan, J. S. Binkley, R. Seeger and J. A. Pople, *J. Chem. Phys.*, 1980, **72**, 650.
- 43 E. Runge and E. K. U. Gross, *Phys. Rev. Lett.*, 1984, **52**, 997.
- 44 M. J. Frisch, G. W. Trucks, H. B. Schlegel, G. E. Scuseria, M. A. Robb, J. R. Cheeseman, G. Scalmani, V. Barone, B. Mennucci, G. A. Petersson, H. Nakatsuji, M. Caricato, X. Li, H. P. Hratchian, A. F. Izmaylov, J. Bloino, G. Zheng, J. L. Sonnenberg, M. Hada, M. Ehara, K. Toyota, R. Fukuda, J. Hasegawa, M. Ishida, T. Nakajima, Y. Honda, O. Kitao, H. Nakai, T. Vreven, J. A. Montgomery, Jr., J. E. Peralta, F. Ogliaro, M. Bearpark, J. J. Heyd, E. Brothers, K. N. Kudin, V. N. Staroverov, R. Kobayashi, J. Normand, K. Raghavachari, A. Rendell, J. C. Burant, S. S. Iyengar, J. Tomasi, M. Cossi, N. Rega, J. M. Millam, M. Klene, J. E. Knox, J. B. Cross, V. Bakken, C. Adamo, J. Jaramillo, R. Gomperts, R. E. Stratmann, O. Yazyev, A. J. Austin, R. Cammi, C. Pomelli, J. W. Ochterski, R. L. Martin, K. Morokuma, V. G. Zakrzewski, G. A. Voth, P. Salvador, J. J. Dannenberg, S. Dapprich, A. D. Daniels, Ö. Farkas, J. B. Foresman, J. V. Ortiz, J. Cioslowski and D. J. Fox, *Gaussian 09 Revision D.01*, Gaussian Inc. Wallingford CT 2009.
- 45 B. O. Roos, P. R. Taylor and P. E. M. Siegbahn, *Chem. Phys.*, 1980, **48**, 157.
- 46 P. E. M. Siegbahn, A. Heiberg, J. Almlöf and B. O. Roos, *J. Chem. Phys.*, 1981, **74**, 2384.
- 47 P. E. M. Siegbahn, A. Heiberg, B. O. Roos and B. Levy, *Phys. Scr.*, 1980, **21**, 323.

- 48 K. Andersson, P.-Å. Malmqvist, B. O. Roos, A. J. Sadlej and K. Wolinski, *J. Phys. Chem.*, 1990, **94**, 5483.
- 49 K. Andersson, P.-Å. Malmqvist and B. O. Roos, *J. Chem. Phys.*, 1992, **96**, 1218.
- 50 R. A. Kendall, T. H. Dunning Jr. and R. J. Harrison, *J. Chem. Phys.*, 1992, **96**, 6796.
- 51 D. E. Woon and T. H. Dunning Jr., *J. Chem. Phys.*, 1993, **98**, 1358.
- 52 F. Aquilante, L. De Vico, N. Ferré, G. Ghigo, P.-Å. Malmqvist, P. Neogrady, T. B. Pedersen, M. Pitoňák, M. Reiher, B. O. Roos, L. Serrano-Andrés, M. Urban, V. Veryazov and R. Lindh, *J. Comput. Chem.*, 2010, **31**, 224.
- 53 J. P. Perdew, K. Burke and H. Ernzerhof, *Phys. Rev. Lett.*, 1996, **77**, 3865.
- 54 J. P. Perdew, K. Burke and H. Ernzerhof, *Phys. Rev. Lett.*, 1997, **78**, 1396.
- 55 P. Deglmann, K. May, F. Furche and R. Ahlrichs, *Chem. Phys. Lett.*, 2004, **384**, 103.
- 56 O. T. K. Eichkorn, H. Öhm, M. Häser and R. Ahlrichs, *Chem. Phys. Lett.*, 1995, **240**, 283.
- 57 M. Sierka, A. Hogekamp and R. Ahlrichs, *J. Chem. Phys.*, 2003, **118**, 9136.
- 58 TURBOMOLE Version 6.6 a Development of University of Karlsruhe and Forschungszentrum Karlsruhe GmbH, 1989-2007, TURBOMOLE GmbH, since 2007; available from <http://www.turbomole.com>.
- 59 A. E. Reed, R. B. Weinstock and F. Weinhold, *J. Chem. Phys.*, 1985, **83**, 735.
- 60 A. E. Reed and F. Weinhold, *J. Chem. Phys.*, 1985, **83**, 1736.
- 61 A. E. Reed, L. A. Curtiss and F. Weinhold, *Chem. Rev.*, 1988, **88**, 899.
- 62 C. Lee, W. Yang and R. Parr, *Phys. Rev. B*, 1988, **37**, 785.
- 63 A. D. Becke, *Phys. Rev. A*, 1988, **38**, 3098.
- 64 B. Miehlich, A. Savin, H. Stoll and H. Preuss, *Chem. Phys. Lett.*, 1989, **157**, 200.
- 65 J. P. Perdew, J. A. Chevary, S. H. Vosko, K. A. Jackson, M. R. Pederson, D. J. Sing and C. Fiolhais, *Phys. Rev. B*, 1992, **46**, 6671.
- 66 A. D. Becke, *J. Chem. Phys.*, 1993, **98**, 5648.
- 67 S. Grimme, J. Antony, S. Ehrlich and H. Krieg, *J. Chem. Phys.*, 2010, **132**, 154104.
- 68 J. P. Perdew, *Phys. Rev. B*, 1986, **33**, 8822.
- 69 Y. Zhao and D. G. Truhlar, *J. Chem. Phys.*, 2006, **125**, 194101.
- 70 Y. Zhao and D. G. Truhlar, *J. Phys. Chem. A*, 2004, **108**, 6908.
- 71 Y. Zhao and D. G. Truhlar, *Theor. Chem. Acc.*, 2008, **120**, 215.
- 72 J.-D. Chai and M. Head-Gordon, *Phys. Chem. Chem. Phys.*, 2008, **10**, 6615.
- 73 T. Yanai, D. P. Tew and N. Handy, *Chem. Phys. Lett.*, 2004, **393**, 51.
- 74 J. M. Nicovich, K. D. Kreutter, C. A. van Dijk and P. H. Wine, *J. Phys. Chem.*, 1992, **96**, 2518.
- 75 *Thermochemical Data of Organic Compounds*, ed. J. B. Pedley, R. D. Naylor and S. Kirby, Chapman and Hall, New York, 1986.
- 76 Y. R. Lee, C. L. Chiu and S. M. Lin, *J. Chem. Phys.*, 1994, **100**, 7376.